



**HAL**  
open science

## **p65/RelA NF- $\kappa$ B fragments generated by RIPK3 activity regulate tumorigenicity, cell metabolism, and stemness characteristics**

Yasmine Touil, Céline Latreche-carton, Hassiba El Bouazzati, Anne-lucie Nugues, Nathalie Jouy, Xavier Thuru, William Laine, Frederic Lepretre, Martin Figeac, Meryem Tardivel, et al.

### ► To cite this version:

Yasmine Touil, Céline Latreche-carton, Hassiba El Bouazzati, Anne-lucie Nugues, Nathalie Jouy, et al. p65/RelA NF- $\kappa$ B fragments generated by RIPK3 activity regulate tumorigenicity, cell metabolism, and stemness characteristics. *Journal of Cellular Biochemistry*, 2022, 123 (3), pp.543-556. 10.1002/jcb.30198 . hal-03641788

**HAL Id: hal-03641788**



**<https://hal.science/hal-03641788v1>**

Submitted on 29 Nov 2022

**HAL** is a multi-disciplinary open access archive for the deposit and dissemination of scientific research documents, whether they are published or not. The documents may come from teaching and research institutions in France or abroad, or from public or private research centers.

L'archive ouverte pluridisciplinaire **HAL**, est destinée au dépôt et à la diffusion de documents scientifiques de niveau recherche, publiés ou non, émanant des établissements d'enseignement et de recherche français ou étrangers, des laboratoires publics ou privés.

# p65/RelA NF- $\kappa$ B fragments generated by RIPK3 activity regulate tumorigenicity, cell metabolism, and stemness characteristics

Yasmine Touil<sup>1,2</sup> | Céline Latreche-Carton<sup>1,2</sup> | Hassiba El Bouazzati<sup>1,2</sup> | Anne-Lucie Nugues<sup>1,2</sup> | Nathalie Jouy<sup>3</sup> | Xavier Thuru<sup>1,2</sup>  | William Laine<sup>1,2</sup> | Frederic Lepretre<sup>3</sup> | Martin Figeac<sup>3</sup> | Meryem Tardivel<sup>3</sup> | Jérôme Kluza<sup>1,2</sup> | Thierry Idziorek<sup>1,2</sup> | Bruno Quesnel<sup>1,2,4</sup> 

<sup>1</sup>CANTHER, UMR 1277 Inserm – 9020 CNRS, University of Lille, Lille, France

<sup>2</sup>Institut pour la Recherche sur le Cancer de Lille, UMR 1277 Inserm – 9020 CNRS, Lille, France

<sup>3</sup>UMS 2014 CNRS/US 41 Inserm, University of Lille, Lille, France

<sup>4</sup>Service des Maladies du Sang, CHU Lille, Lille, France

## Correspondence

Thierry Idziorek, Inserm, UMR 1277 Inserm – 9020 CNRS, 59000 Lille, France.  
Email: [thierry.idziorek@inserm.fr](mailto:thierry.idziorek@inserm.fr)

Bruno Quesnel, Service des Maladies du Sang, Center Hospitalier et Universitaire de Lille, Rue Polonovski, 59037, Lille, France.

Email: [bruno.quesnel@chru-lille.fr](mailto:bruno.quesnel@chru-lille.fr)

## Funding information

Institut National Du Cancer, Grant/Award Number: INCa-DGOS-Inserm 6041aa; Institut pour la Recherche sur le Cancer de Lille, Grant/Award Number: Institut pour la Recherche sur le Cancer de Lille

## Abstract

Receptor-interacting protein kinase 3 (RIPK3) can induce necroptosis, apoptosis, or cell proliferation and is silenced in several hematological malignancies. We previously reported that RIPK3 activity independent of its kinase domain induces caspase-mediated p65/RelA cleavage, resulting in N-terminal 1-361 and C-terminal 362-549 fragments. We show here that a noncleavable p65/RelA D361E mutant expressed in DA1-3b leukemia cells decreases mouse survival times and that co-expression of p65/RelA fragments increases the tumorigenicity of B16F1 melanoma cells. This aggressiveness in vivo did not correlate with NF- $\kappa$ B activity measured in vitro. The fragments and p65/RelA D361E mutant induced different expression profiles in DA1-3b and B16F1 cells. Stemness markers were affected: p65/RelA D361E increased ALDH activity in DA1-3b cells, and fragment expression increased melanoma sphere formation in B16/F1 cells. p65/RelA fragments and the D361E noncleavable mutant decreased oxidative or glycolytic cell metabolism, with differences observed between models. Thus, p65/RelA cleavage initiated by kinase-independent RIPK3 activity in cancer cells is not neutral and induces pleiotropic effects in vitro and in vivo that may vary across tumor types.

## KEYWORDS

cancer, fragment, p65/RelA, RIPK3, stemness

Thierry Idziorek and Bruno Quesnel should be considered joint senior authors.

This is an open access article under the terms of the Creative Commons Attribution-NonCommercial-NoDerivs License, which permits use and distribution in any medium, provided the original work is properly cited, the use is non-commercial and no modifications or adaptations are made.

© 2021 The Authors. *Journal of Cellular Biochemistry* Published by Wiley Periodicals LLC

## 1 | INTRODUCTION

Receptor-interacting protein kinase 3 (RIPK3, RIP3) associated with RIPK1 in a necrosome complex that can induce necroptosis, apoptosis, or cell proliferation.<sup>1</sup> We previously reported decreased RIPK3 expression in the majority of examined acute myeloid leukemia (AML) patients.<sup>2</sup> These results were confirmed by Hockendorf et al.,<sup>3</sup> who demonstrated that RIPK3 restricts malignant myeloproliferation by activating the inflammasome, promoting cell differentiation and death, and that loss of RIPK3 increases the leukemic burden in mice. Alteration of the necrosome complex in hematological malignancies has also been reported in chronic lymphocytic leukemia (CLL), in which decreased expression of RIPK3 and CYLD has been found to cause decreased sensitivity to tumor necrosis factor- $\alpha$  (TNF- $\alpha$ ).<sup>4</sup> The oncogenic effects of MYC may also be partially mediated through inhibition of the RIPK3/RIPK1 interaction.<sup>5</sup> Thus, RIPK3 plays an important role in tumorigenicity regulation in hematological malignancies, and researchers have also suggested a role for RIPK3 in lung cancers, colon cancers, and melanoma.<sup>6–8</sup>

We also previously reported that re-expression of a RIPK3 mutant with an inactive kinase domain (RIPK3-kinase dead [RIPK3-KD]) significantly increased apoptosis and resulted in earlier apoptosis in comparison with the effects induced by wild-type RIPK3 (RIPK3-WT), indicating that the RIPK3 kinase domain is an essential regulator of apoptosis/necroptosis in leukemia cells.<sup>2</sup> Inducing the expression of RIPK3-KD, but not RIPK3-WT, in vivo prolonged the survival of mice injected with leukemia cells. The expression of RIPK3-KD induced caspase-dependent p65/RelA nuclear factor- $\kappa$ B (NF- $\kappa$ B) subunit cleavage, and a non-cleavable p65/RelA D361E mutant (Figure S1) rescued these cells from apoptosis. This cleavage, partially mediated by caspase-6, was abolished through an aspartate-to-glutamate substitution at D361 within the *INFD* site. The p65/RelA N-terminal 1-361 and C-terminal 362-549 fragments generated by p65/RelA cleavage in RIPK3-KD-expressing cells had no effect on cell survival in vitro. NF- $\kappa$ B regulation through p65/RelA cleavage by caspase-3 after chemotherapy, viral infection, or cytokine deprivation and dominant-negative effects of p65/RelA fragments on NF- $\kappa$ B transcriptional activity have been reported.<sup>9–13</sup> In contrast, RIPK3-KD-generated p65/RelA fragments have been found to have enhanced NF- $\kappa$ B transcriptional activity.<sup>2</sup> Thus, RIPK3 has kinase-independent proapoptotic activity and mediates p65/RelA cleavage, but the precise role of p65/RelA fragments remains unclear.

Here, we report that in mouse models of leukemia and melanoma, the noncleavable p65/RelA D631E mutant or p65/RelA fragments enhance tumorigenicity. In addition, coexpression of p65/RelA fragments induces

distinct transcriptomic profiles and modulates stemness markers and cell metabolism mechanisms, indicating that RIPK3-mediated p65/RelA cleavage may profoundly modify essential tumor cell characteristics.

## 2 | MATERIALS AND METHODS

### 2.1 | Reagents and antibodies

Antibodies against the Myc tag on NF- $\kappa$ B p65/RelA (D14E12) XP were purchased from Cell Signaling Technologies. Human/mouse anti-RelA/NF- $\kappa$ B p65 and the rat IgG2A isotype control (54447) [Alexa Fluor<sup>®</sup> 647] antibodies were purchased from R&D Systems. The His-tagged mAb was purchased from Novagen. The donkey anti-sheep IgG H&L (Alexa Fluor<sup>®</sup> 488) (ab150177) antibody was purchased from Abcam. The Alexa Fluor 514-conjugated goat anti-mouse IgG (H + L) cross-adsorbed secondary antibody and the Alexa Fluor 647-conjugated goat anti-rabbit IgG (H + L) cross-adsorbed secondary antibody were purchased from Thermo Fisher Scientific. For confocal microscopy, anti-tag antibodies were used at a final dilution of 1:100, the human/mouse anti-RelA/NF- $\kappa$ B p65 antibody was used at a final dilution of 1:20, and all of the secondary antibodies were used at a 1:500 dilution.

### 2.2 | Cell lines

The leukemic murine DA1-3b p210<sup>BCR-ABL</sup> cell line and the DA1-3b/C3H/HeOuJ mouse model were maintained as previously described.<sup>14–16</sup> B16F1 murine melanoma cells were acquired from ATCC (CRL-1619TM; CRL 6323TM) and maintained as previously described.<sup>17</sup> B16F1 cells were chosen as an additional model sufficiently distinct from the DA1-3b leukemia model to explore the possible general effects of p65/RelA fragments.

### 2.3 | Plasmids and p65/RelA mutants

The mouse p65/RelA D361E cDNA mutant and fragments have been previously described (Figure S1).<sup>2</sup> The p65/RelA D361E mutant was generated by mutating the *INFD* putative consensus recognition site for caspase-6. The p65/RelA 1-361 fragment was generated with a His-tag at its 3' end, and the p65 362-549 fragment was generated with a Myc tag at its 5' end. After transfection of DA1-3b or B16F1 cells, stable cell lines were obtained via selection with blasticidin, and the cells were sorted with an ARIA III cell sorter (Becton Dickinson) according to DsRed fluorescence.

## 2.4 | In vivo studies

Eight-week-old C3H/HeOuj female mice (Charles River Laboratories) were injected intraperitoneally (IP) with  $5 \times 10^6$  DA1-3b/Void, DA1-3b/p65/RelA WT, DA1-3b/p65/RelA D361E, or DA1-3b/p65/RelA 1-361 + p65/RelA 362-549 cells. The same experiment was also performed with Swiss nude mice Crl:NU (NCR)-Foxn1<sup>nu</sup> (Charles River Laboratories) injected IP with  $1 \times 10^5$  cells. Animal experiments were approved by the Animal Care Ethical Committee CEEA. NPDC (agreement no. 2017022716306305).

To study the ability of B16F1 melanoma cells stably transduced with the same cDNA as the DA1-3b cells to form tumors, 50 000 cells (200  $\mu$ l) were subcutaneously injected into 8-week-old C57BL/6Jrj immunocompetent mice. Tumor growth was assessed at the indicated time points by performing bidimensional measurements with a caliper. Tumor volumes in mm<sup>3</sup> were calculated using the following formula: width<sup>2</sup>  $\times$  length  $\times$  0.5.

## 2.5 | Measurement of NF- $\kappa$ B activity

The phosphorylation level of NF- $\kappa$ B p65/RelA at Ser468 and Ser536 was detected using a FACE NF- $\kappa$ B kit (Active Motif) according to the manufacturer's instructions. A  $\kappa$ B-luc reporter containing three  $\kappa$ B-binding sites and negative control plasmids was kindly provided by Dr. Isabelle Vanseuning. <sup>18</sup> Five million cells were transfected with the NF- $\kappa$ B reporter vector or a negative control vector. A reporter assay was performed using a Dual-Glo<sup>®</sup> Luciferase Assay System (Promega) according to previously published methods. The DNA-binding activities of NF- $\kappa$ B p50, p62, and p65/RelA in nuclear extracts were measured using TransAM NF- $\kappa$ B p65/RelA and TransAM NF- $\kappa$ B Family Kits (Active Motif) according to the manufacturer's instructions.

## 2.6 | Transcriptome analysis

Total RNA was prepared using an RNeasy mini-kit (Qiagen) according to the manufacturer's instructions, including the additional DNase treatment step. Total RNA yield and quality were further assessed on an Agilent 2100 bioanalyzer (Agilent Technologies). One color, whole mouse (028005 slides), 60-mer oligonucleotide, and  $8 \times 60$ k microarrays (Agilent Technologies) were used to analyze gene expression. cRNA labeling, hybridization, and detection were performed according to the manufacturer's instructions (Agilent Technologies). For each microarray, Cy3-labeled cRNA

was synthesized with a low-input QuickAmp labeling kit from 50 ng of total RNA. RNA Spike-In was added to all tubes as a positive control for labeling and amplification steps. The labeled cRNA was purified, and 600 ng of each cRNA was then hybridized and washed as per the manufacturer's instructions. Microarrays were scanned on an Agilent G2505C scanner, and data were extracted using Agilent Feature Extraction Software<sup>®</sup> (FE version 10.7.3.1).

The microarray data are available from the NCBI GEO depository (accession no. GSE98437). Statistical comparisons and filtering were achieved with Genespring<sup>®</sup> software version GX13.0 (Agilent Technologies).

## 2.7 | Measurement of ALDH<sup>+</sup> cells

Quantification of ALDH<sup>+</sup> cells was achieved with an ALDEFLUOR<sup>™</sup> Kit (Stem Cell) according to the manufacturer's instructions using an LSR-X20 flow cytometer (BD Biosciences).

## 2.8 | Sphere formation assay

To generate spheres,  $4 \times 10^3$  transduced B16F1 cells were plated on 24-well plates coated with a 0.5 mg/ml poly-2-hydroxyethylmetacrylate (polyHEMA) ethanol solution (Sigma-Aldrich) to prevent cell attachment and cultured in 1 ml of Dulbecco's modified Eagle's medium (DMEM)/F12 medium (Gibco<sup>®</sup>, Life Technologies<sup>™</sup>) supplemented with 20 ng/ml EGF (Stem Cells Biotechnologies), 1:50 B27 supplement (Gibco<sup>®</sup>, Invitrogen<sup>™</sup>), and 20 ng/ml rHu bFGF (PromoKine-PromoCell GmbH) in a humidified 5% CO<sub>2</sub> incubator at 37°C for 7 days. The cell density was maintained at 4 cells per  $\mu$ l to prevent cell aggregation. Spheres (comprising more than ~50 cells) were counted under an inverted microscope.

## 2.9 | Assessment of oxygen consumption and extracellular pH

Cells were seeded in XFe24 plates (Agilent; Les Ulis, France) at  $20\text{--}40 \times 10^3$  cells/well and  $150 \times 10^3$  cells/well for the B16F1 and DA1-3B cell lines, respectively. Oxygen consumption rates (OCRs) and extracellular acidification rates (ECARs) were measured using an XFe24 Extracellular Flux Analyzer (Corazao-Rozas et al. (2013)). Briefly, media containing treatments were removed, and cells were washed once with DMEM supplemented with 10 mM glucose, 2 mM glutamine,

and 1 mM pyruvate at pH 7.4. The cells were incubated at 37°C in the absence of CO<sub>2</sub> for 1 h. Baseline OCR measurements were determined before administration of oligomycin (1 μM), 2-[2-(3-chlorophenyl) hydrazinylydene] propanedinitrile (FCCP; 0.25–0.5 μM), and a combination of antimycin A and rotenone (0.5 μM; AA/Rot.). Measurements were normalized against cell concentrations.

## 2.10 | Statistics

All data were analyzed using SigmaPlot 13 software (SYSTAT).

## 3 | RESULTS

### 3.1 | p65/RelA fragments and a noncleavable p65/RelA D361E mutant modulate tumorigenicity in leukemia and melanoma mouse models

We previously showed that RIPK3-KD expression in leukemia cells induced cleavage at D361 of the p65/RelA NF-κB subunit, partially due to caspase-6 activity.<sup>2</sup> Interestingly, the noncleavable p65/RelA D361E mutant rescued leukemic cells from apoptosis, suggesting that it plays a major role in survival pathways. We, therefore, investigated how the absence of p65/RelA cleavage or the expression of fragments resulting from cleavage at D361 could affect mouse survival in a DA1-3b mouse leukemia model.<sup>15,19</sup> Injection of DA1-3b cells expressing the p65/RelA D361E mutant (designated DA1-3b/p65D361E, Figure S1) into C3HeOuJ mice significantly reduced mouse survival rates (Figure 1A). Coexpression of the p65/RelA N-terminal 1-361 and C-terminal 362-549 fragments (designated DA1-3b/p65 1-361 + 362-549) conferred leukemogenicity similar to that observed with p65/RelA WT expression (designated DA1-3b/p65 WT) (Figure 1B). To avoid the influence of immunogenicity induced by the p65/RelA D361E mutant protein or fragments, we then injected immunodeficient nude mice with the same cell lines. Again, DA1-3b/p65D361E cells showed significantly increased tumorigenicity. Because the NF-κB pathway is highly activated by p210<sup>BCR-ABL</sup> in DA1-3b cells, which may render them more susceptible to p65/RelA fragment modulation, we also evaluated tumorigenicity in the B16F1 melanoma tumor model.<sup>14,17</sup> We transduced B16F1 mouse melanoma cells with the same p65/RelA NF-κB fragment, wild-type, and void control plasmids. Tumor growth was increased in mice injected with B16F1/p65 1-361 + 362-549, B16F1/p65 1-361, and B16F1/p65 WT cells compared with that in mice injected with B16F1/Void, B16F1/p65D361E, or B16F1/p65 362-549 cells (Figure 1C).

Thus, coexpression of p65/RelA fragments yielded aggressive melanoma cells *in vivo*. The effect of the noncleavable D361E mutant appeared to be opposite in leukemia versus melanoma cells.

These results indicate that p65/RelA fragments are not inactive by-products of RIPK3 activity and may differentially modulate tumorigenicity across tumor types.

### 3.2 | Modulation of p65/RelA NF-κB nuclear translocation by p65/RelA fragments

To better understand the role of p65/RelA fragments, we first analyzed the cytoplasmic and nuclear localization of the constructs in transfected DA1-3b cells. A p65/RelA 1-361 fragment and p65/RelAD361E mutant were generated with a His-tag at the C-terminus, and the p65 362-549 fragment was generated with a Myc tag at the N-terminus to allow their specific identification (Figure S1). As depicted in Figure 2, control DA1-3b/Void cells showed endogenous p65/RelA expression in the cytoplasmic and nuclear compartments. In DA1-3b/p65 WT cells, the p65/RelA protein was detected in the cytoplasmic compartment with all three antibodies, while the noncleavable p65/RelA D361E mutant was found in the cytoplasm using anti-p65/RelA and anti-Myc antibodies and in the nucleus using an anti-His antibody, suggesting that some protein cleavage occurred through alternate sites. The p65/RelA 1-361 fragment bearing the nuclear localization sequence (NLS) was mostly found in the cytoplasm, suggesting that this moiety alone cannot enter the nucleus. The p65/RelA 362-549 fragment bearing the transcription activity domain (TAD) was mainly found in the nucleus, suggesting that it may be aided by the endogenous NF-κB complex. Surprisingly, in DA1-3b/p65 1-361 + 362-549 cells, the 1-361 fragment was mostly found in the cytoplasm, while the 362-549 fragment was equally distributed between the cytoplasm and nucleus, indicating that the former prevented the latter from entering the nucleus, as nuclear localization was observed when only the 1-361 fragment was present. These data indicate that p65/RelA fragments are able to translocate into the nucleus, similar to the full-length protein. The findings also suggest that there are possible interactions between the fragments.

### 3.3 | Transcriptional activity of p65/RelA fragments

To further investigate the activity of p65/RelA fragments in tumor cells, we first investigated the phosphorylation levels of Ser467 (mouse homolog of human Ser468) and Ser534 (mouse homolog of human Ser536) using a FACE

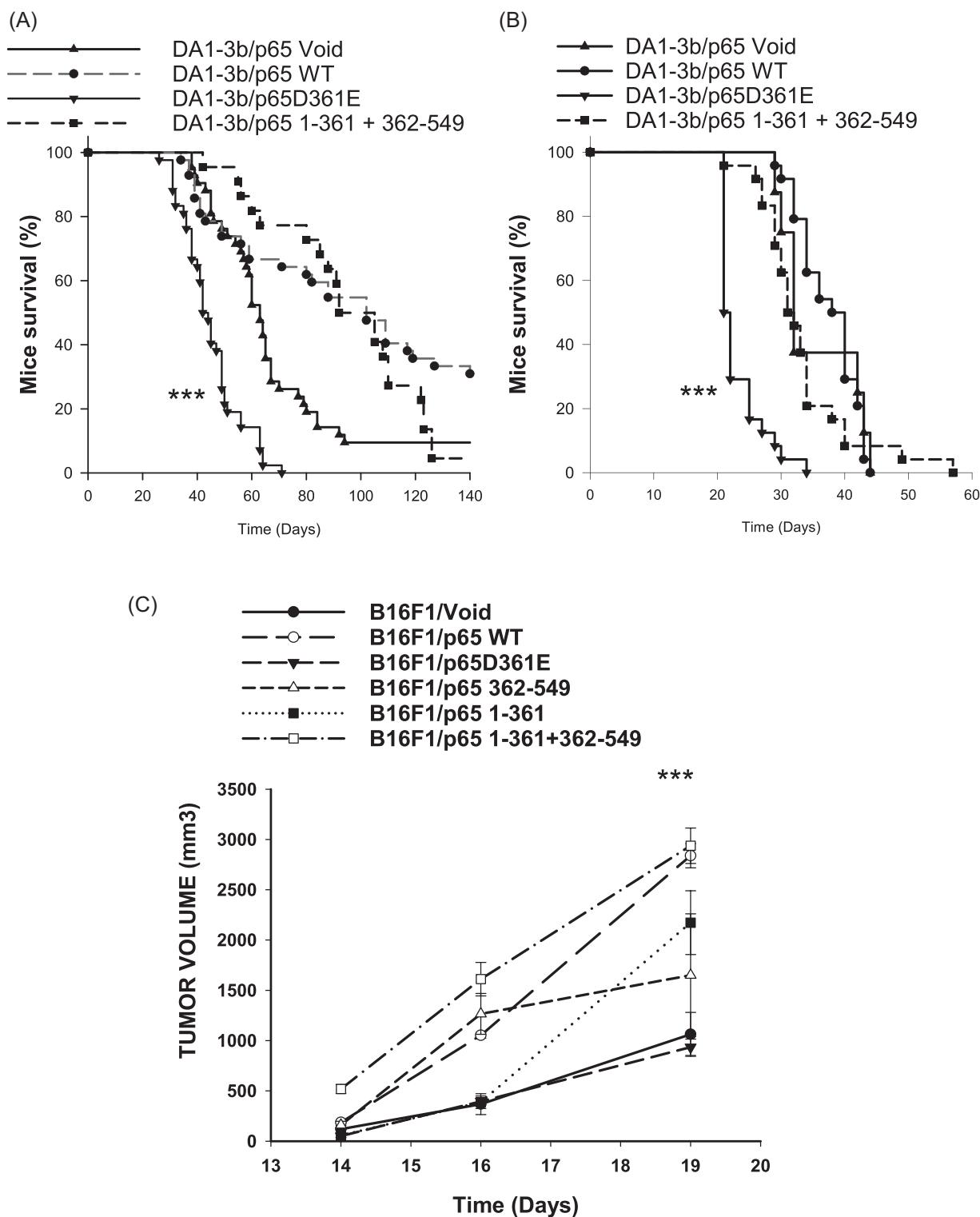


**FIGURE 1** Tumorigenicity of p65/RelA mutants in DA1-3b leukemia and B16/F1 melanoma cells. (A) Survival of syngeneic C3H/HeOuJ mice intraperitoneally (IP) injected with  $5 \times 10^6$  DA1-3b/p65 WT, DA1-3b/p65D361E or DA1-3b/p65 1-361 + 362-549 cells (10 mice/group). Statistical analysis was performed using a log-rank test. (B) Survival of Swiss nude mice injected intraperitoneally with  $1 \times 10^5$  DA1-3b/p65WT, DA1-3b/p65D361E, or DA1-3b/p65 1-361 + 362-549 cells (8 mice/group). (C) Tumor volume of syngeneic C57BL/6 mice injected intraperitoneally with  $1 \times 10^5$  B16F1/Void, B16F1/p65 WT, B16F1/p65D361E, B16F1/p65 1-361, B16F1/p65 362-549 or B16F1/p65 1-361 + 362-549 cells (8 mice/group). Statistical analysis was performed using Student's *t*-test. \*\*\* $<.001$

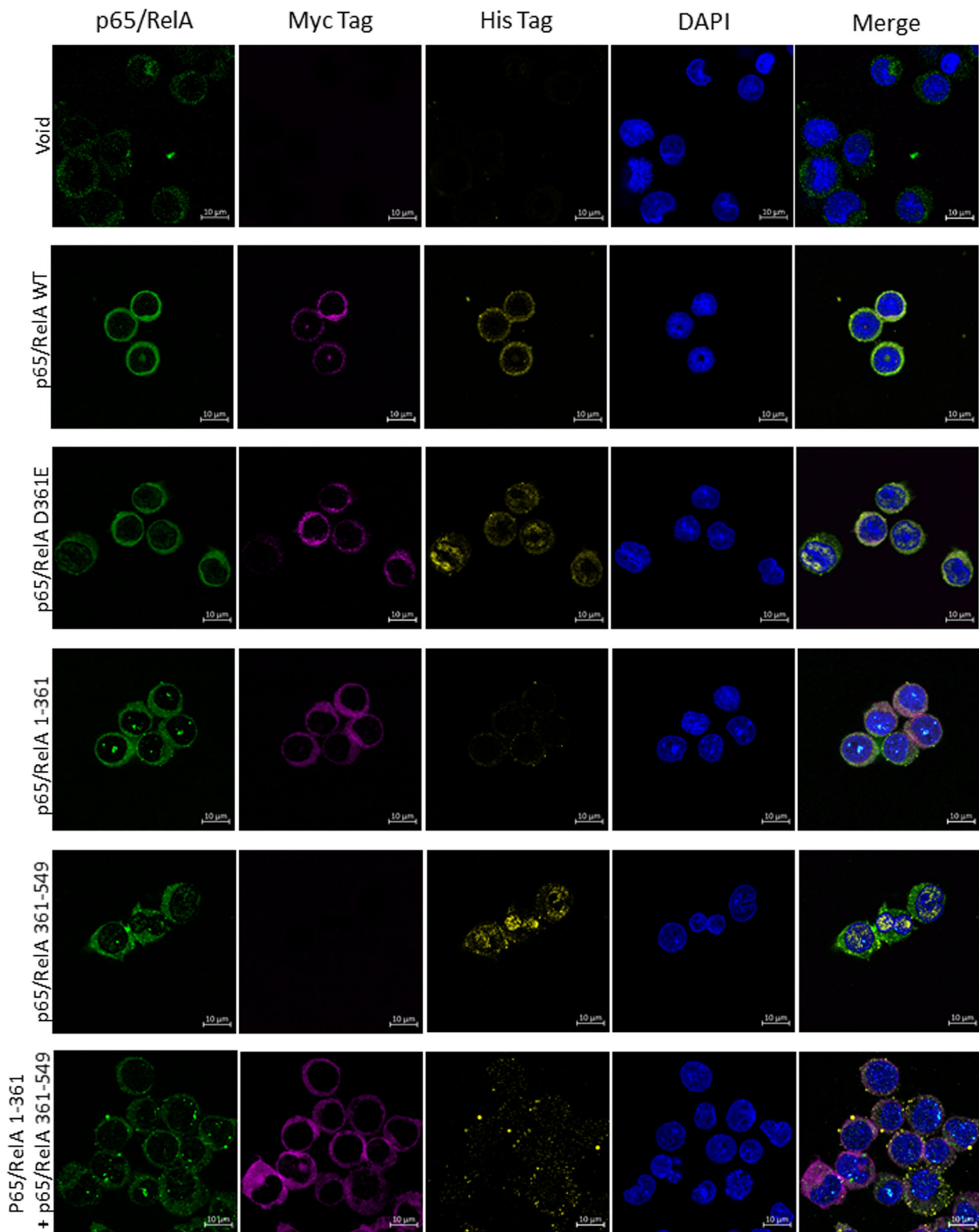


**FIGURE 2** Subcellular localization of WT p65/RelA and mutants. The different constructs were tagged with Myc at the C-terminus and His at the N-terminus. Confocal microscopy images of DA1-3b cells expressing the Void plasmid, p65/RelA WT, p65/RelA D361E, p65/RelA 1-361, p65/RelA 361-549, or p65/RelA 1-361 + 361-549 and stained with anti-His, anti-Myc, and anti-p65/RelA antibodies and DAPI. Bars represent 10  $\mu\text{m}$  under 63 $\times$  magnification. Cells are representative of three independent experiments

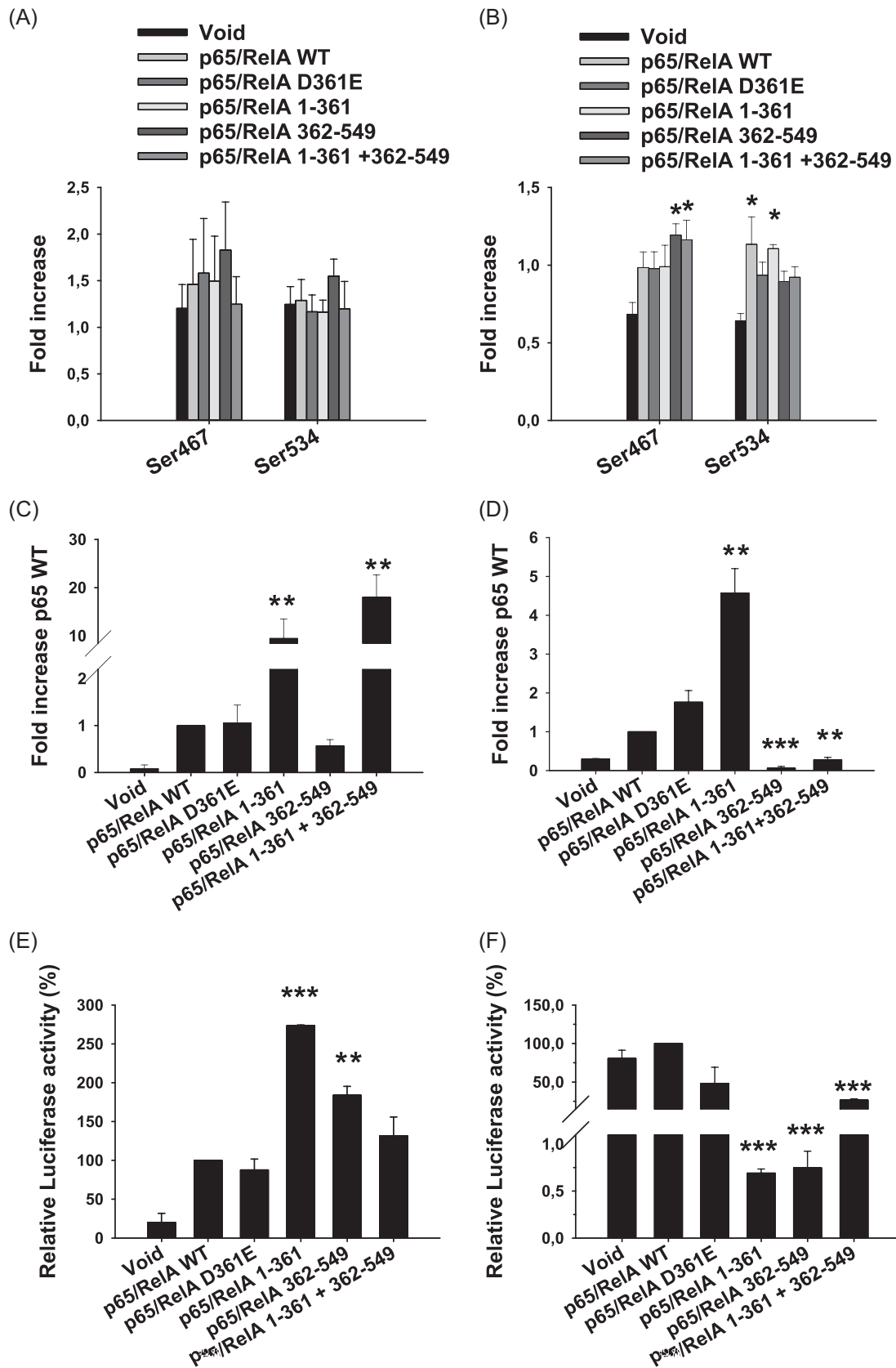


FIGURE 3 (See caption on next page)



in-cell western blot analysis system. No significant differences between p65/RelA fragments, the D361E noncleavable mutant, and full-length protein were observed in DA1-3b (Figure 3A) or B16F1 cells (Figure 3B). In B16F1 cells, each p65/RelA protein exhibited increased Ser467 and Ser534 phosphorylation compared with that of control B16F1/Void cells. However, no significant differences were observed between the fragments, the mutant, and the wild-type protein, indicating that the p65/RelA fragments and the D361E mutant do not differentially affect p65/RelA phosphorylation at these sites. We then measured the amount of NF- $\kappa$ B p65/RelA bound to consensus DNA-binding sites using a TransAM assay (Active Motif). Nuclear extracts from DA1-3b/p65 WT and DA1-3b/p65 D361E cells showed similar p65/RelA binding (Figure 3C). However, nuclear extracts from DA1-3b/p65 1-361 and notably DA1-3b/p65 1-361 + 362-549 cells demonstrated significantly enhanced binding. Conversely, in B16F1 melanoma cells, the coexpression of p65/RelA fragments resulted in reduced p65/RelA binding activity, and the D361E mutant and p65/RelA 1-361 showed the highest binding activity (Figure 3D). Analyses of other components of NF- $\kappa$ B, namely, p50, p52, and RelB, revealed no differences (except for p52, although the difference was not significant) in DA1-3b cells expressing the fragments (Figure S2). To further explore the hypothesis that p65/RelA fragments modulate NF- $\kappa$ B activity, we analyzed the transcriptional activity of NF- $\kappa$ B using a  $\kappa$ B-luc reporter plasmid.<sup>18</sup> In DA1-3b cells (Figure 3E), NF- $\kappa$ B activity increased in the presence of p65/RelA fragments, whereas in B16F1 cells (Figure 3F), the lowest NF- $\kappa$ B activity level was observed in cells expressing the isolated fragments. Thus, the increased tumorigenicity induced by the noncleavable p65/RelA D361E mutant in DA1-3b leukemia cells and the coexpressed p65/RelA fragments in the B16F1 model cannot be explained by modulation of NF- $\kappa$ B activity.

### 3.4 | Transcriptomic analysis of DA1-3b cells expressing p65/RelA fragments and the noncleavable D361E mutant

Because the p65/RelA fragments and noncleavable D361E mutant did not appear to mediate tumorigenicity through

conventional NF- $\kappa$ B activity, we investigated possible new functions through transcriptomic profile analyses of DA1-3b and B16F1 cells. The microarray data are available from the NCBI GEO depository (accession nos. GSE135136 and GSE135137 for DA1-3b and B16 cells, respectively). Unsupervised clustering (Figure 4) allowed the perfect stratification of mutants of these lineages, and differentially expressed genes were identified by limma analysis using R. Limma analysis of probe intensities with filters fixed at Pabs<0.01 and Fcabs>2 revealed 102 (40 upregulated and 62 downregulated) and 158 (111 upregulated and 47 downregulated) highly differentially expressed genes in B16 and DA1-3B cells, respectively.

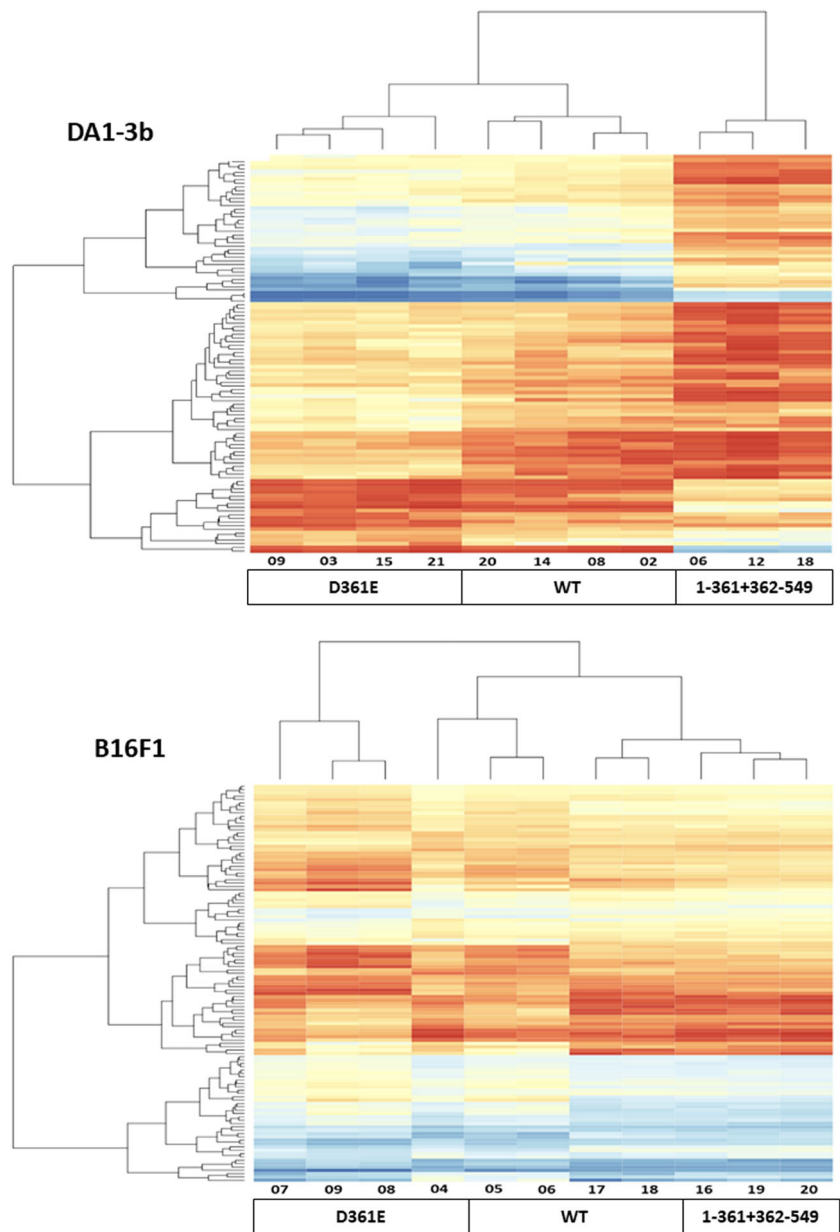
A subsequent Ingenuity Pathway Analysis (IPA, Qiagen®) revealed the involvement of these differentially expressed genes in several diseases and biological functions, including cancer (adjusted *p*-value: 2.34E−04), hypoxia-inducible factor signaling (adjusted *p*-value: 1.63E−02) and hematological system development and function (adjusted *p*-value: 1.63E−02) (Figures S3 and S4). IPA confirmed these results with similar molecular and cellular functions (cellular function and maintenance, cell-to-cell signaling and interaction, cellular movement, cellular growth and proliferation and development, with adjusted *p*-values ranging from 1.78E−24 to 4.67E−15 in DA1-3b/p65/RelA 1-361 + 362-549 vs. DA1-3b/p65/RelA WT cells). Physiological system development involved hematological system development and function (adjusted *p*-value: 9.97E−21), immune cell trafficking (adjusted *p*-value: 1.52E−19), and hematopoiesis (adjusted *p*-value: 3.08E−14). Disease analysis revealed the involvement of inflammatory response and immunological disease pathways, with an adjusted *p*-value of approximately 2E−19. Thus, p65/RelA fragments and the D361E mutant induced specific transcriptomic profiles.

### 3.5 | p65/RelA fragments regulate stemness characteristics

The NF- $\kappa$ B pathway plays a role in multiple cancer cell processes, including stemness.<sup>20</sup> We investigated the

**FIGURE 3** NF- $\kappa$ B activity of p65/RelA WT and mutants. (A) p65/RelA Ser467 and Ser534 phosphorylation measured with a FACE assay in DA1-3b cells expressing the Void plasmid, p65/RelA WT, p65/RelA D361E, p65/RelA 1-361, p65/RelA 362-549, or p65/RelA 1-361 + 362-549. (B) Same as (A) but for B16F1 cells. (C) Quantification of the p65/RelA NF- $\kappa$ B complex DNA-binding activity in nuclear extracts from DA1-3b cells expressing the Void plasmid, p65/RelA WT, p65/RelA D361E, p65/RelA 1-361, p65/RelA 362-549, or p65/RelA 1-361 + 362-549. (D) Same as (C) but for B16F1 cells. (E) Transcriptional activity of the different p65/RelA fragments and D361E mutant evaluated using an NF- $\kappa$ B-luc reporter system in DA1-3b and (F) B16F1 cells. Three independent experiments were conducted, and statistical analysis was performed using Student's *t*-test. \**p* < .05, \*\**p* < .01, and \*\*\**p* < .001

**FIGURE 4** Transcriptomic analysis of p65/RelA WT and mutant targets in DA1-3b leukemic cells and B16F1 melanoma cells. Genespring unsupervised hierarchical clustering of DA1-3b/p65/RelA WT, DA1-3b/p65/RelA and DA1-3b/p65/RelA 1-361 + 362-549 cells (upper panel) and B16F1/p65/RelA WT, B16F1/p65/RelA and B16F1/p65/RelA 1-361 + 362-549 cells (lower panel)



influence of p65/RelA fragments on stemness characteristics in DA1-3b and B16F1 cells. Aldehyde dehydrogenase (ALDH) activity has been found to be a reliable hematopoietic stem cell (HSC) marker and may also define leukemia stem cells (LSCs) in some AML patients.<sup>21–25</sup> ALDH activity measured by flow cytometry with Aldefluor was significantly higher in DA1-3b cells expressing the p65/RelA D361E mutant than in cells expressing p65/RelA WT or the fragments, which did not demonstrate different ALDH levels (Figure 5A). ALDH activity has also been proposed to be marker of stemness in melanoma; however, inconsistent results have been observed across studies.<sup>26</sup> Here, ALDH activity was significantly lower in B16F1 cells expressing the p65/RelA D361E mutant than in cells expressing p65/RelA WT or the fragments

(Figure 5B and Supplementary Figure S5). Sphere formation has been found to be a stemness marker in melanoma.<sup>17,27,28</sup> B16F1 cells expressing p65/RelA D361E formed significantly fewer spheres than control cells and cells expressing p65/RelA WT or coexpressing the fragments (Figure 5C). Thus, the p65/RelA fragments may influence certain tumor stemness characteristics in different ways across tumor types.

### 3.6 | p65/RelA fragments regulate oxidative metabolism

Cancer stem cells are composed of a large population of quiescent cells that display specific metabolic characteristics. For instance, low levels of oxidative

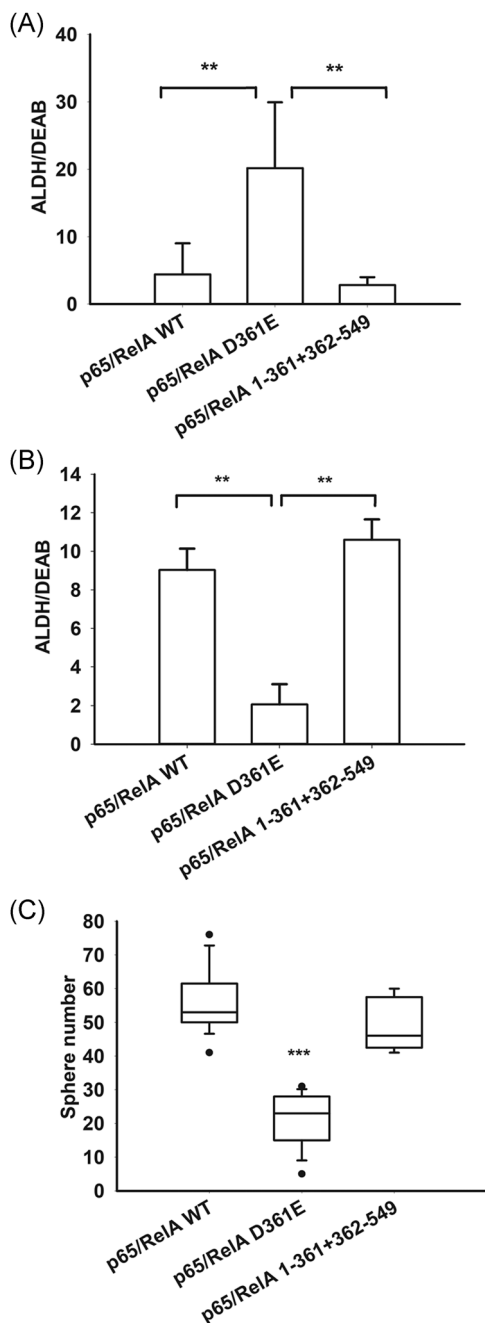


**FIGURE 5** Modulation of stemness markers by the p65/RelA mutant and fragments. (A) Measurement of ALDH activity using flow cytometry with Aldefluor in DA1-3B/p65/RelA WT, p65/RelA D361E, and p65/RelA/1-361 + 362-549 cells. Values represent the MFI ratio of cells incubated with Aldefluor and cells incubated with DEAB and Aldefluor. (B) Same as (A) but for B16F1 cells. (C) Quantification of the number of spheres in B16F1/Void, p65/RelA WT, p65/RelA D361E, and p65/RelA 1-361 + 362-549 melanoma cells. Bars represent the mean value of 18 independent experiments. \* $p < .05$ , \*\* $p < .01$  and \*\*\* $p < .001$ , using Student's *t*-test

phosphorylation and glycolysis are observed in myeloid leukemia stem cells. As p65/RelA mutants affect the expression of stemness markers in DA1-3b and B16F1 cells, we assessed cellular metabolism changes in response to these mutants.

OCRs were measured in leukemic DA1-3B and melanoma B16F1 cells expressing the p65/RelA mutants. Analyses of basal and maximal respiration indicated that the mutants behaved differently between the two cell lines (Figure 6A,B). Among the DA1-3B p65/RelA mutant cells, the groups with the highest respiratory activity were DA1-3b p65/RelA Void and WT cells. p65/RelA 1-361 + 362-549 yielded intermediate activity, while the p65/RelA D361E mutant-expressing cells had the lowest overall oxygen consumption rate (Figure 6A). These mutants behaved differently in melanoma B16F1 cells (Figure 6B). B16F1 cells transfected with the Void plasmid displayed the highest activity, while B16 p65/RelA 1-361 + 362-549 yielded a modest reserve capacity and maximal respiration. B16F1 p65/RelA WT- and D361E-transfected cells displayed minimal cellular energetics. Our results indicate differences in oxidative metabolism in response to the mutants between the two cell lines, except for the response to p65/RelA D361E, which induced very low mitochondrial respiration in both leukemic and melanoma models.

Quantification of extracellular acidification (the basal ECAR) as a measure of glycolytic turnover was also carried out and plotted against the basal OCR to check for metabolic potential (Figure 6C,D). DA1-3b cells expressing the Void and mutant plasmids demonstrated an energetic phenotype (high levels of OCR and ECAR). B16F1 cells expressing the Void plasmid displayed an aerobic phenotype, whereas those expressing p65/RelA WT, 1-361/362-549, and D361E mutants were sequentially less metabolic and showed a more quiescent phenotype (lower level of glycolysis and mitochondrial respiration).

Overall, the metabolic potential of B16F1 melanoma cells reflects their ability to behave as quiescent stem cells. However, these effects were not observed in DA1-3B leukemia cells, highlighting the phenotypic differences between the two models (Figure 5). Additionally, the results indicate that p65/RelA fragment expression decreases energetic metabolism.

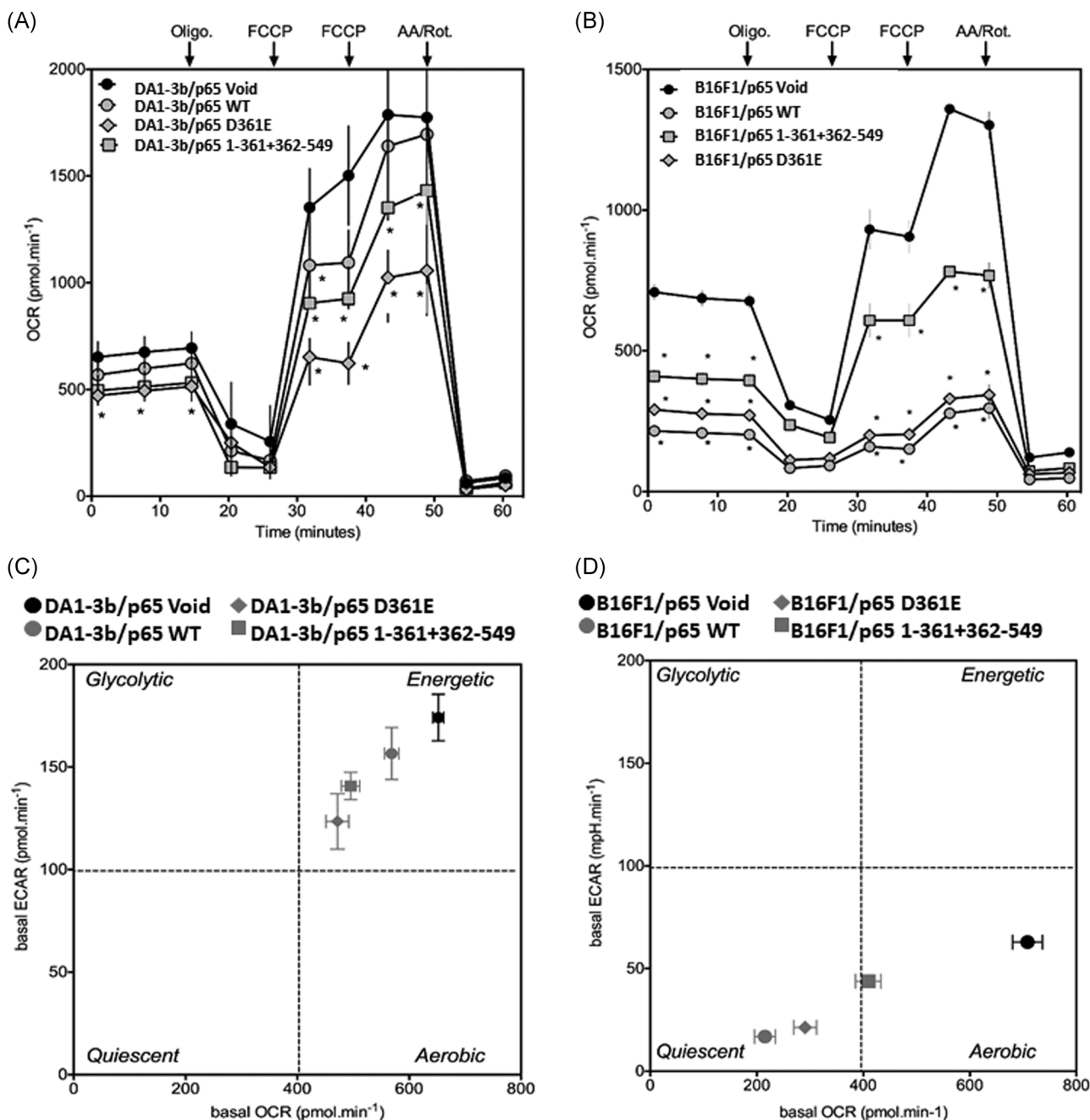


**FIGURE 6** Oxygen consumption and extracellular pH of leukemic and melanoma cell lines transfected with the p65/RelA mutant and fragments. Oxygen consumption rates (OCRs) and extracellular acidification rates (ECARs) were measured using an XFe24 Extracellular Flux Analyzer. The left (A, C) and right panels (B, D) correspond to leukemic DA1-3B and melanoma B16F1 cell lines, respectively, expressing p65/RelA Void, p65/RelA WT, p65/RelA D361E, and p65/RelA 1-361 + 362-549. Dots and bars represent the means and errors of ten measurements. Nonvisible bars indicate that the values are smaller than the size of the dot. Statistical analysis was performed using the log-rank test; \* $p < .05$

## 4 | DISCUSSION

Regulation of NF- $\kappa$ B by caspase-dependent cleavage of p65/RelA has been described under various conditions.<sup>9–13</sup> The intrinsic activity of p65/RelA fragments generated in this manner has only been partially investigated, with reports suggesting possible dominant-

negative effects.<sup>10,12</sup> We previously described new p65/RelA fragments produced by the kinase-independent activity of RIPK3, mediated at least partially by caspase-6.<sup>2</sup> We also reported that RIPK3 is silenced in the vast majority of AML patients, a finding confirmed by another group, suggesting that p65/RelA cleavage mediated by RIPK3 may be absent in some tumors.<sup>3</sup> However,

the role of p65/RelA fragments and whether their absence provides any benefit to tumor cells remains unknown.

Here, we show that p65/RelA fragments modulate tumorigenicity, although differently across tumor types. In DA1-3b leukemic cells, the p65/RelA D361E noncleavable mutant shortened mouse survival times. This result confirms and expands upon our previous finding that p65/RelA D361E rescues DA1-3b cells from apoptosis. Thus, in leukemia cells, silencing the p65/RelA cleavage induced by RIPK3 is likely to promote tumorigenicity. In B16F1 melanoma cells, in which RIPK3 is not silenced, as observed in our previous transcriptomic study of this cell line (GEO accession number GSE69703), the effects on tumorigenicity were almost inverted.<sup>17</sup> Coexpressed fragments were highly tumorigenic, while the noncleavable p65/RelA D361E mutant had no effect. To the best of our knowledge, this is the first observation of tumorigenicity modulated by products resulting from p65/RelA cleavage activity. However, the distinct effects of the noncleavable mutant and fragments in the two different tumor models are puzzling and suggest a more complex role for p65/RelA cleavage than modulation of NF- $\kappa$ B activity alone. It must also be noted that although mouse melanoma B16F1 cells express RIPK3, silencing of this gene has been reported in several other melanoma cell lines and tumors, indicating that B16F1 cells may be representative of only a fraction of human melanoma cells.<sup>8</sup>

To investigate how p65/RelA fragments enhanced tumorigenicity, we investigated their effect on NF- $\kappa$ B activity. Fragments translocated into the nucleus similarly to the full-length protein when they were coexpressed and dramatically enhanced p65/RelA DNA binding to NF- $\kappa$ B consensus sites in DA1-3b cells. This enhanced binding was not observed in B16F1 cells. However, this enhanced binding did not result in significantly enhanced or reduced NF- $\kappa$ B transcriptional activity, which suggests that modulation of tumorigenicity by the fragments is not the result of NF- $\kappa$ B pathway activity but perhaps of other functions.

p65/RelA fragments and the noncleavable p65/RelA D361E mutant induced clearly distinct transcriptomic profiles, clearly establishing that the fragments are active and are not inert byproducts of RIPK3-induced, caspase-mediated cleavage. The fragments and the noncleavable mutant modulated (in opposite ways) several genes that are not known as specific NF- $\kappa$ B pathway targets.

The role of the NF- $\kappa$ B pathway in cancer stemness has been the subject of conflicting reports.<sup>29,30</sup> NF- $\kappa$ B is thought to be a major link between inflammation and cancer stemness. NF- $\kappa$ B activation by pro-inflammatory cytokines or TLR ligands increases stemness in some

models, and cancer stem cells show increased NF- $\kappa$ B activity.<sup>31</sup> For instance, a CD34+ subpopulation of AML cells has been shown to exhibit high NF- $\kappa$ B activity.<sup>32</sup> However, in other tumor types, NF- $\kappa$ B inhibition was found to enhance cancer stem cell expansion.<sup>33</sup> We observed here that stemness markers were modulated by p65/RelA fragments and the mutant in both models. p65/RelA D361E increased ALDH activity in DA1-3b cells and reduced sphere formation in B16/F1 melanoma cells. Conversely, coexpressed p65/RelA fragments induced reduced ALDH activity in DA1-3b cells and increased sphere formation in B16F1 cells. These results are consistent with the observed *in vivo* tumorigenicity of the DA1-3b and B16F1 cell models. However, the p65/RelA WT and Void did not induce sphere formation capacity changes in B16F1 cells despite promoting substantial differences in tumorigenicity. Energetic metabolism was also modulated by p65/RelA fragments. p65/RelA fragments and the D361E noncleavable mutant decreased oxidative or glycolytic cell metabolism differently between the models. Tumor stem cell metabolism has been characterized as low in different tumor types. These findings suggest that p65/RelA cleavage may play a role that is distinct from the effect of p65/RelA WT on some cancer stemness markers in certain tumor types, but this function needs to be investigated further.

Our results indicate that p65/RelA fragments generated by RIPK3 kinase-independent activity are not neutral; instead, these fragments induce pleiotropic effects in cancer cells, including effects associated with stemness, metabolism, and tumorigenicity that may vary across tumor types. These effects do not appear to be solely related to modulation of classical NF- $\kappa$ B transcriptional activity. All these findings need to be interpreted cautiously. The functions of the p65/RelA fragments reported here were studied in stably transduced cancer cells. We previously observed the generation of p65/RelA cleavage and related fragments in leukemia cells expressing RIPK3-KD, in which this protein induces substantial early apoptosis.<sup>2</sup> In such a situation, some of the effects mediated by p65/RelA fragments may be transient, and we currently do not know whether these fragments are stably present in nonapoptotic cancer cells. In addition, it must be noted that the only known alteration mechanism of RIPK3 in cancer is silencing, notably in AML and CLL, suggesting that p65/RelA fragment functions would be absent. Notably, here, expression of the noncleavable D361E mutant yielded DA1-3b leukemic cells with the highest tumorigenicity. p65/RelA fragments may also play a role in cancer cells in which RIPK3 is expressed and activated, possibly via inflammatory stimuli from the microenvironment, such as through TNF- $\alpha$  stimulation. In support of this hypothesis, we observed

enhanced tumorigenicity in a melanoma model. Further investigation is needed to determine the precise roles of p65/RelA fragments in cancer.

## ACKNOWLEDGMENTS

This study was supported by the SIRIC OncoLille, grant number INCa-DGOS-Inserm 6041aa, and Institut pour la Recherche sur le Cancer de Lille. We are grateful to Isabelle Vanseuning for providing the  $\kappa$ B-luc reporter and Céline Villenet and Shéhérazade Sebda for array production. We thank Bernadette Masselot, Pascaline Segard, and Antonino Bongiovani for technical assistance.

## CONFLICT OF INTERESTS

The authors declare that there are no conflict of interests.

## AUTHOR CONTRIBUTIONS

Bruno Quesnel and Thierry Idziorek designed the study. Céline Latreche-Carton, Yasmine Touil, Nathalie Jouy, Hassiba El Bouazzati, Anne-Lucie Nugues, Xavier Thuru, Jérôme Kluza, William Laine, and Martin Figeac performed the research and analyzed the data. Yasmine Touil, Céline Latreche-Carton, Thierry Idziorek, and Bruno Quesnel wrote the paper.

## DATA AVAILABILITY STATEMENT

The microarray data are available through the NCBI GEO depository (accession nos. GSE135136 and GSE135137 for DA1-3b and B16 cells, respectively).

## ORCID

Xavier Thuru  <http://orcid.org/0000-0002-0998-4160>

Bruno Quesnel  <http://orcid.org/0000-0002-6563-2709>

## REFERENCES

- Weinlich R, Oberst A, Beere HM, Green DR. Necroptosis in development, inflammation and disease. *Nat Rev Mol Cell Biol*. 2017;18(2):127-136. doi:10.1038/nrm.2016.149
- Nugues AL, El Bouazzati H, Hetuin D, et al. RIP3 is down-regulated in human myeloid leukemia cells and modulates apoptosis and caspase-mediated p65/RelA cleavage. *Cell Death Dis*. 2014;5:e1384. doi:10.1038/cddis.2014.347
- Hockendorf U, Yabal M, Herold T, et al. RIPK3 restricts myeloid leukemogenesis by promoting cell death and differentiation of leukemia initiating cells. *Cancer Cell*. 2016;30(1):75-91. doi:10.1016/j.ccell.2016.06.002
- Liu P, Xu B, Shen W, et al. Dysregulation of TNF $\alpha$ -induced necroptotic signaling in chronic lymphocytic leukemia: suppression of CYLD gene by LEF1. *Leukemia*. 2012;26(6):1293-1300. doi:10.1038/leu.2011.357
- Seong D, Jeong M, Seo J, et al. Identification of MYC as an antinecrotic protein that stifles RIPK1-RIPK3 complex formation. *Proc Natl Acad Sci U S A*. 2020;117(33):19982-19993. doi:10.1073/pnas.2000979117
- Moriwaki K, Bertin J, Gough PJ, Orlowski GM, Chan FK. Differential roles of RIPK1 and RIPK3 in TNF-induced necroptosis and chemotherapeutic agent-induced cell death. *Cell Death Dis*. 2015;6:e1636. doi:10.1038/cddis.2015.16
- Fukasawa M, Kimura M, Morita S, et al. Microarray analysis of promoter methylation in lung cancers. *J Hum Genet*. 2006;51(4):368-374. doi:10.1007/s10038-005-0355-4
- Geserick P, Wang J, Schilling R, et al. Absence of RIPK3 predicts necroptosis resistance in malignant melanoma. *Cell Death Dis*. 2015;6:e1884. doi:10.1038/cddis.2015.240
- Kang KH, Lee KH, Kim MY, Choi KH. Caspase-3-mediated cleavage of the NF-kappa B subunit p65 at the NH2 terminus potentiates naphthoquinone analog-induced apoptosis. *J Biol Chem*. 2001;276(27):24638-24644. doi:10.1074/jbc.M101291200
- Levkau B, Scatena M, Giachelli CM, Ross R, Raines EW. Apoptosis overrides survival signals through a caspase-mediated dominant-negative NF-kappa B loop. *Nat Cell Biol*. 1999;1(4):227-233. doi:10.1038/12050
- Neuzil J, Schroder A, von Hundelshausen P, et al. Inhibition of inflammatory endothelial responses by a pathway involving caspase activation and p65 cleavage. *Biochemistry*. 2001;40(15):4686-4692. doi:10.1021/bi002498n
- Coiras M, Lopez-Huertas MR, Mateos E, Alcami J. Caspase-3-mediated cleavage of p65/RelA results in a carboxy-terminal fragment that inhibits IkappaBalpha and enhances HIV-1 replication in human T lymphocytes. *Retrovirology*. 2008;5:109. doi:10.1186/1742-4690-5-109
- Neznanov N, Chumakov KM, Neznanova L, Almasan A, Banerjee AK, Gudkov AV. Proteolytic cleavage of the p65-RelA subunit of NF-kappaB during poliovirus infection. *J Biol Chem*. 2005;280(25):24153-24158. doi:10.1074/jbc.M502303200
- Joha S, Nugues AL, Hetuin D, et al. GILZ inhibits the mTORC2/AKT pathway in BCR-ABL(+) cells. *Oncogene*. 2012;31(11):1419-1430. doi:10.1038/onc.2011.328
- Saudemont A, Buffenoir G, Denys A, et al. Gene transfer of CD154 and IL12 cDNA induces an anti-leukemic immunity in a murine model of acute leukemia. *Leukemia*. 2002;16(9):1637-1644. doi:10.1038/sj.leu.2402590
- Saudemont A, Hamrouni A, Marchetti P, et al. Dormant tumor cells develop cross-resistance to apoptosis induced by CTLs or imatinib mesylate via methylation of suppressor of cytokine signaling 1. *Cancer Res*. 2007;67(9):4491-4498. doi:10.1158/0008-5472.CAN-06-1627
- Touil Y, Segard P, Ostyn P, et al. Melanoma dormancy in a mouse model is linked to GILZ/FOXO3A-dependent quiescence of disseminated stem-like cells. *Sci Rep*. 2016;6:30405. doi:10.1038/srep30405
- Skrypek N, Duchene B, Hebbar M, Leteurtre E, van Seuning I, Jonckheere N. The MUC4 mucin mediates gemcitabine resistance of human pancreatic cancer cells via the concentrative nucleoside transporter family. *Oncogene*. 2013;32(13):1714-1723. doi:10.1038/onc.2012.179
- Saudemont A, Quesnel B. In a model of tumor dormancy, long-term persistent leukemic cells have increased B7-H1 and B7.1 expression and resist CTL-mediated lysis. *Blood*. 2004;104(7):2124-2133. doi:10.1182/blood-2004-01-0064
- Huang G, Wen Q, Zhao Y, Gao Q, Bai Y. NF-kappaB plays a key role in inducing CD274 expression in human monocytes after lipopolysaccharide treatment. *PLoS One*. 2013;8(4):e61602. doi:10.1371/journal.pone.0061602

21. Hoang VT, Hoffmann I, Borowski K, et al. Identification and separation of normal hematopoietic stem cells and leukemia stem cells from patients with acute myeloid leukemia. *Methods Mol Biol.* 2013;1035:217-230. doi:10.1007/978-1-62703-508-8\_19
22. Smith C, Gasparetto M, Humphries K, Pollyea DA, Vasilios V, Jordan CT. Aldehyde dehydrogenases in acute myeloid leukemia. *Ann N Y Acad Sci.* 2014;1310:58-68. doi:10.1111/nyas.12414
23. Gerber JM, Smith BD, Ngwang B, et al. A clinically relevant population of leukemic CD34(+)/CD38(-) cells in acute myeloid leukemia. *Blood.* 2012;119(15):3571-3577. doi:10.1182/blood-2011-06-364182
24. Gerber JM, Zeidner JF, Morse S, et al. Association of acute myeloid leukemia's most immature phenotype with risk groups and outcomes. *Haematologica.* 2016;101(5):607-616. doi:10.3324/haematol.2015.135194
25. Hoang VT, Buss EC, Wang W, et al. The rarity of ALDH(+) cells is the key to separation of normal versus leukemia stem cells by ALDH activity in AML patients. *Int J Cancer.* 2015;137(3):525-536. doi:10.1002/ijc.29410
26. Boonyaratanakornkit JB, Yue L, Strachan LR, et al. Selection of tumorigenic melanoma cells using ALDH. *J Invest Dermatol.* 2010;130(12):2799-2808. doi:10.1038/jid.2010.237
27. Dou J, Pan M, Wen P, et al. Isolation and identification of cancer stem-like cells from murine melanoma cell lines. *Cell Mol Immunol.* 2007;4(6):467-472. <https://www.ncbi.nlm.nih.gov/pubmed/18163959>
28. Touil Y, Zuliani T, Wolowczuk I, et al. The PI3K/AKT signaling pathway controls the quiescence of the low-Rhodamine123-retention cell compartment enriched for melanoma stem cell activity. *Stem Cells.* 2013;31(4):641-651. doi:10.1002/stem.1333
29. Shigdar S, Li Y, Bhattacharya S, et al. Inflammation and cancer stem cells. *Cancer Lett.* 2014;345(2):271-278. doi:10.1016/j.canlet.2013.07.031
30. Wang T, Shigdar S, Gantier MP, et al. Cancer stem cell targeted therapy: progress amid controversies. *Oncotarget.* 2015;6(42):44191-44206. doi:10.18632/oncotarget.6176
31. Guzman ML, Neering SJ, Upchurch D, et al. Nuclear factor-kappaB is constitutively activated in primitive human acute myelogenous leukemia cells. *Blood.* 2001;98(8):2301-2307. doi:10.1182/blood.v98.8.2301
32. Yeh, DW, Huang LR, Chen YW, Huang CF, Chuang TH. Interplay between inflammation and stemness in cancer cells: the role of Toll-like receptor signaling. *J Immunol Res.* 2016;2016:4368101-4368114. doi:10.1155/2016/4368101
33. Liu M, Sakamaki T, Casimiro MC, et al. The canonical NF-kappaB pathway governs mammary tumorigenesis in transgenic mice and tumor stem cell expansion. *Cancer Res.* 2010;70(24):10464-10473. doi:10.1158/0008-5472.CAN-10-0732

### SUPPORTING INFORMATION

Additional supporting information may be found in the online version of the article at the publisher's website.

**How to cite this article:** Touil Y, Latreche-Carton C, Bouazzati HE, et al. p65/RelA NF- $\kappa$ B fragments generated by RIPK3 activity regulate tumorigenicity, cell metabolism, and stemness characteristics. *J Cell Biochem.* 2022;123:543-556. doi:10.1002/jcb.30198